2-Substituted-Naphthalene Binary and Ternary Systems: From Random Alloys to Complexes

Alain Marbeuf,*,† Didier Mikaïlitchenko,† Philippe Negrier,† Miquel-Angel Cuevas-Diarte,‡ and Teresa Calvet-Pallas‡

Centre de Physique Moléculaire Optique et Hertzienne, UMR 5798 CNRS, Université Bordeaux I, 33405 Talence Cedex, France, and Departament de Cristallografia, Universitat de Barcelona, Marti i Franquès 08028 Barcelona, Spain

Received March 21, 2000. Revised Manuscript Received July 10, 2000

2-Chloronaphthalene−octafluoronaphthalene, 2-methylnaphthalene−octafluoronaphthalene binary systems and 2-chloronaphthalene−2-methylnaphthalene−octafluoronaphthalene ternary system have been assessed by differential scanning calorimetry and X-ray powder diffraction. Each binary system presents a 1:1 complex. The pseudobinary section of the ternary system shows a new phase which is probably ordered and may behave as a "complex of complexes". Finally, ternary alloys show the turn over from ordered to random lattices. Thermodynamic properties of these systems are analyzed through the associated liquid model and the line-compound formalism.

1. Introduction

As in metallic binary systems, organic binaries $A_{1-x}B_x$ are known to give either random or ordered alloys: the former mixed lattices correspond to random molecular alloys between pure substances and depend on the degree of isomorphism, which is related to the molecular shape and size, and on the crystalline isomorphism (related to the similarity of symmetry).[1−4] For binary mixtures of Lennard-Jones hard spheres, it has been recently shown that geometric (Lennard-Jones diameter ratio) and energetic criteria (well-depth ratio) can explain random alloy stability.[5] The ordered molecular alloys are often called complexes: the formation of ordered phases results from specific attractive interactions, such as charge transfer between molecules of different type[6] or quadrupole λ-quadrupole interactions.[7] By applying a modified pairwise approach to different molecular substances and their binary alloys, we have very recently shown that complex formation occurs when a stabilizing effect affects heteromolecular energy and overcompensates homomolecular energies, which is not the case for random alloys.[8]

Our research on molecular complexes is part of a wider program on mixed molecular interactions. To date we have published on the formation of ordered alloys (1:1 complex phases) between a substituted benzene, $R_mR'_nC_6H_{6-m-n}$ (R, R′ = H, Cl, CH_3), and hexafluorobenzene, C_6F_6:[9−11] (i) the complex existence is related to the planar geometry of each molecular partner and the presence of H···F intermolecular interactions, and (ii) a strong relationship is found between complex stability and association character in the liquid. With the naphthalene−octafluoronaphthalene system,[12] our purpose was to extend these basic ideas to naphthalene systems, with octafluoronaphthalene playing the same role as C_6F_6.

On the other hand, chlorine appears to destabilize benzene complex phases more than hydrogen and methyl group. By studying naphthalene binary systems where one hydrogen is substituted by a chlorine atom (2-chloronaphthalene−octafluoronaphthalene system) or by a methyl group (2-methylnaphthalene−octafluoronaphthalene system), we attempt to determine whether the relation between the nature of the substitute and the stability of the complex is maintained.

Given that a maximum appears in the 2-chloronaphthalene−2-methylnaphthalene solid−liquid equilibrium phase diagram, for 2-chloronaphthalene-rich compositions,[13] we search for a possible transition from random alloys to complexes, by studying the ternary system

* To whom correspondence should be addressed. Phone: +(33) 5-56-84-83-56. Fax: +(33) 5-56-84-66-86. E-mail: marbeuf@frbdx11.cribx1.u-bordeaux.fr.

† Université Bordeaux I.

‡ Universitat de Barcelona.

(1) Haget, Y.; Oonk, H. A. J.; Cuevas-Diarte, M. A. In *Les Equilibres entre Phases, JEEP XVI.*; Kaloustian, J., Pastor, J., Eds.; Marseille, 1990; pp 35−36.

(2) Haget, Y.; Bonpunt, L.; Michaud, F.; Négrier, P.; Cuevas-Diarte, M. A.; Oonk, H. A. J. *J. Appl. Crystallogr.* **1990**, *23*, 492.

(3) Oonk, H. A. J.; van der Linde, P. R.; Haget, Y.; Bonpunt, L.; Chanh, N. B.; Cuevas-Diarte, M. A. *J. Chim. Phys.* **1991**, *88*, 329.

(4) Haget, Y. *J. Chim. Phys.* **1993**, *90*, 313.

(5) Hitchcock, M. A.; Hall, C. K. *J. Chem. Phys.* **1999**, *110*, 11433.

(6) Forster, R. Organic Charge-Transfer Complexes; Blomquist, A. T., Ed.; Academic Press: London, 1969, Chapter 10, pp 276−299.

(7) Hernandez-Trujillo, J.; Costas, M.; Vela, A.. *J. Chem. Soc., Faraday Trans.* **1993**, *89*, 2441.

(8) Marbeuf, A.; Mikaïlitchenko, D.; Würger, A.; Oonk, H. A. J.; Cuevas-Diarte, M. A. *Phys. Chem. Chem. Phys.* **2000**, *2*, 261.

(9) Marbeuf, A.; Mondieig, D.; Métivaud, V.; Négrier, P.; Cuevas-Diarte, M. A.; Haget, Y. *J. Mol. Cryst. Liq. Cryst.* **1997**, *293*, 309.

(10) Mikaïlitchenko, D.; Marbeuf, A.; Haget, Y.; Oonk, H. A. J. *J. Mol. Cryst. Liq. Cryst.* **1998**, *319*, 291.

(11) Mikaïlitchenko, D.; Marbeuf, A.; Oonk, H. A. J. *Chem. Mater.* **1999**, *11* (10), 2866.

(12) Michaud, F.; Négrier, P.; Mikaïlitchenko, D.; Marbeuf, A.; Haget, Y.; Cuevas-Diarte, M. A.; Oonk, H. A. J. *J. Mol. Cryst. Liq. Cryst.* **1999**, *326*, 409.

(13) Calvet-Pallas, T.; Cuevas-Diarte, M. A.; Haget, Y.; Mondieig, D.; Kok, I. C.; Verdonk, M. L.; van Miltenburg, J. C.; Oonk, H. A. J. *J. Chem. Phys.* **1999**, *10*, 4841.

10.1021/cm001046u CCC: $19.00
Published on Web 10/11/2000

built with 2-chloronaphthalene, 2-methylnaphthalene, and octafluoronaphthalene: in other words, we examine the connection between intermolecular interactions and order/disorder.

To this end we have (i) determined and analyzed 2-chloronaphthalene−octafluoronaphthalene and 2-methylnaphthalene−octafluoronaphthalene systems and (ii) studied the 2-chloronaphthalene−2-methylnaphthalene−octafluoronaphthalene system. Experimental procedure and thermodynamics are presented, with special emphasis on the associated liquid model used in thermodynamic analysis. Pure component, binary, and ternary data are reported and discussed.

2. Experimental Procedure and Thermodynamic Analysis

Calorimetric measurements giving transition temperatures and enthalpies, (such as solid−solid transition temperature and enthalpy, T_{trs} and $\Delta_{trs}H$, respectively, and melting temperature and enthalpy, T_{fus} and $\Delta_{fus}H$, respectively) were performed with a Perkin-Elmer DSC7 differential scanning calorimeter. The temperature range was between 160 and 320 K and all our experiments were carried out with the same procedure as in ref 10: heating or cooling rate, 2 K/min; sample mass ≈ 4 mg. Uncertainties are estimated by taking into account a systematic apparatus contribution (0.2 K and 1% for enthalpy measurements) and a random part using the Student's method with a 95% threshold of reliability.

To characterize the different phases and their transitions, (space group, lattice parameters and volume, kind of the transitions), X-ray diffractions patterns are obtained with a Guinier-Simon camera (GS), Siemens D500 or Inel CPS120 (Cu Kα1 radiation, $\lambda = 1.5406$ Å). Space group and related lattice parameters are proposed from indexing diffraction patterns and refinement of peak positions by using the "FULLPROF" routine.[14] The excess volume, $\Delta_{xs}V_\varphi$, of an alloy φ, with general formula $A_{1-x\varphi}B_{x\varphi}$, is a direct measure of the departure from ideality and is immediately deduced from the volume values of A and B, $V_{A,\varphi}$ and $V_{B,\varphi}$ respectively:

$$\Delta_{xs}V_\varphi = V_{\varphi\lambda-}(1 - x_\varphi)V_{A,\varphi\lambda-}x_\varphi V_{B,\varphi} \quad (1)$$

By combining all these experimental methods, the $T-x$ phase diagram can be determined in each system. The corresponding data set is analyzed through appropriated models for each phase, that is, the substituted solution model (SSM), and, if necessary, the associated solution model (ASM) for the liquid. All these models describe excess thermodynamic properties through analytical forms of Gibbs free energy, $\Delta_{mix}G_\varphi$, and related functions (mixing enthalpy, $\Delta_{mix}H_\varphi$, excess entropy, $\Delta_{xs}S_\varphi$). For a given phase φ corresponding to a ternary mixture $A_{x1,\varphi}B_{x2,\varphi}D_{x3,\varphi}$, where $x_{1,\varphi}$, $x_{2,\varphi}$, and $x_{3,\varphi}$ correspond respectively to the mole fraction of the A, B, and D components, SSM argues that components i are randomly distributed; if an interpolation of the Muggianu-type,[15] between binary properties, is made, without ternary interaction terms, $\Delta_{mix}G_\varphi$ takes the following form, at a given temperature, T

$$\Delta_{mix}G_\varphi = \sum_{i=1}^{2}\sum_{j>i}^{3}(\Delta_{mix}H_{ij,\varphi} - T\Delta_{xs}S_{ij,\varphi}) + RT\sum_{i=1}^{3}x_{i,\varphi}\ln x_{i,\varphi} \quad (2)$$

where R is the gas constant, and where the ij binary functions are given by:

$$\Delta_{mix}H_{ij,\varphi} = x_{i,\varphi}x_{j,\varphi}\sum_{v=1}^{n}H_{ij,\varphi}^{(v)}(x_{i,\varphi} - x_{j,\varphi})^{v-1} \quad (3)$$

$$\Delta_{xs}S_{ij,\varphi} = x_{i,\varphi}x_{j,\varphi}\sum_{v=1}^{n}S_{ij,\varphi}^{(v)}(x_{i,\varphi} - x_{j,\varphi})^{v-1}$$

Equations 3 correspond to Redlich−Kister polynomia forms[16] and v is generally restricted to the values 1 (regular approximation) or 2 (subregular approximation). For solid-phase φ, it is more convenient to refer the Gibbs free energy to the pure liquid components, by using the adequate free energy of formation of these components, $\Delta_fG°_{i,\varphi}$, or of the corresponding line-compounds (complexes), $\Delta_fG_{ij,\varphi}$, if φ is a pseudobinary alloy $A_{1-x\varphi}D_{x\varphi}$:B between complexes ($ij$ = A:B, D:B). As an example:

$$\Delta_fG°_{ij,\varphi} = \alpha_{ij,\varphi} - \beta_{ij,\varphi}T + \delta_{ij,\varphi}T(1 - \ln T) \quad (4)$$

where $\alpha_{ij,\varphi}$, $\beta_{ij,\varphi}$, and $\delta_{ij,\varphi}$ are constants, $\delta_{ij,\varphi}$ corresponding to a possible change in heat capacity $\Delta C_{P,\,ij,\,\varphi}$.

The Gibbs free energy of a mixed solid-phase φ is then expressed as

$$\Delta G_{ij,\varphi} = \Delta_{mix}G_\varphi + \sum_{i=1}^{3}x_{i,\varphi}\Delta_fG°_{i,\varphi} \quad (5)$$

or

$$\Delta G_\varphi = \Delta_{mix}G_\varphi + (1-x_\varphi)\Delta_fG°_{13,\varphi} + x_\varphi\Delta_fG°_{23,\varphi} \quad (6)$$

Equation 5 corresponds to random alloys and eq 6 to a pseudobinary alloy between complexes.

In the ASM approach, liquid is assumed to contain uncombined species and associates, i. Therefore, a ternary liquid will contains fives species [three uncombined species, A, D, B, and two associates, (A:B) and (D:B)], which are numbered consecutively 1 through 5 and whose mole fractions are denoted as y_i.[17,18] These species are in chemical equilibrium:

$$(A:B) \Leftrightarrow A + B,\ (D:B) \Leftrightarrow D + B$$

and interact in such a way that mixing Gibbs free energy is now expressed as:

$$\Delta_{mix}G_L = \{\sum_{i=1}^{4}\sum_{j>i}^{5}[y_iy_j\sum_{v=1}^{2}(H_{ij}^{(v)} - TS_{ij}^{(v)})(y_i - y_j)^{v-1}] + (H_{123} - TS_{123})\} - \sum_{j=4}^{5}y_i(\Delta_{diss}H_i - T\Delta_{diss}S_i) + RT\sum_{i=1}^{5}y_i\ln y_i \quad (7)$$

After dividing by the quantity $(1 + y_4 + y_5)$, $\Delta_{mix}G_L$ becomes really a molar quantity. As in eq 2, a Muggianu interpolation between binary excess functions is made, but in eq 7 (i) ternary interactions are taken into account by the term $(H_{123} - TS_{123})$ and (ii) the dissociation energy of the associates, $(\Delta_{diss}H_i - T\Delta_{diss}S_i)$, means that $\Delta_{mix}G_L$ is referred to the pure liquid components.

Thus, the thermodynamic analysis of the complete data set and the calculation of the phase diagram can be achieved through "BIMING" or "TERMING" routines (binary or ternary systems, respectively).[12,19]

3. Results and Discussion

3.1. Pure Components: 2-$C_{10}H_7Cl$, 2-$C_{10}H_7CH_3$, and $C_{10}F_8$. *a. Octafluoronaphthalene (or $C_{10}F_8$).* The

(14) Rodriguez-Carjaval, J. "FULLPROF" routine In *Abstracts of the Satellite Meeting on Powder Diffraction of the XVth Congress of the International Union of Crystallography*; Rodriguez-Carjaval, J., Ed.; Toulouse, 1990, 127.

(15) Muggianu, Y. M.; Gambino, M.; Bros, J. P. *J. Chim. Phys.* **1975**, *72*, 83.

(16) Redlich, O.; Kister, A. T. *Ind. Eng. Chem.* **1948**, *40*, 345.

(17) Tung, T.; Su, C. H.; Liao, P. K.; Brebrick, R. F. *J. Vac. Sci. Technol.* **1982**, *21*, 117.

(18) Marbeuf, A.; Druihle, R.; Triboulet, R.; Patriarche, G. *J. Cryst. Growth* **1992**, *117*, 10.

(19) Marbeuf, A. "BIMING" and "TERMING" routines, Agence Nationale du Logiciel, Paris, 1991.

Table 1. Crystallographic Characteristics of the Pure Components

	octafluoronaphthalene		2-chloronaphthalene		2-methylnaphthalene	
phase	II [20]	I [12]	II [2]	I [2]	III [22]	I [22]
a (Å)	11.287(11)	11.963(17)	7.750(5)	7.662(5)	6.082(4)	7.798(3)
b (Å)	4.674(36)	5.023(10)	5.970(5)	5.994(5)	7.800(4)	5.976(4)
c (Å)	17.033(27)	7.622(20)	21.344(8)	10.650(8)	20.133(14)	10.732(7)
β (Å)	107.34(57)	96.77(6)	119.88(4)	120.32(4)	120.36(5)	119.66(5)
group	$P2_1/a$	$P2_1/a$	$P2_1/a$	$P2_1/a$	$P2_1/a$	$P2_1/a$
Z	4	2	4	2	4	2
T (K)	260	293	293	323	273	293

Table 2. Thermodynamic Data of the Pure Components[a]

	octafluoronaphthalene	2-chloronaphthalene	2-methylnaphthalene
T_{fus}	358.8 ± 0.4	330.7 ± 0.4	306.9 ± 0.5
$\Delta_{fus}H$	17550 ± 330	13940 ± 400	11800 ± 500
$T_{trs,II\rightarrow I}$	283.6 ± 1.3	313.1 ± 0.5	292.0 [22]
$\Delta_{trs}H_{II\rightarrow I}$	2120 ± 100		
$T_{trs,III\rightarrow II}$			289.5 [22]

[a] Temperatures are given in K and enthalpies in J mol^{-1}.

Table 3. Comparison Experiments-Optimization of Thermodynamic Data for the 2-Chloronaphthalene−Octafluoronaphthalene System (SI units)

	experimental values	optimized values
liquid		$H_{13}^{(1)} = 0$ $S_{13}^{(1)} = 1.4(4)$ $H_{13}^{(2)} = 0$ $S_{13}^{(2)} = 0$ $H_{14}^{(1)} = 1080(10)$ $S_{14}^{(1)} = 7.9(8)$ $H_{34}^{(1)} = 330(10)$ $S_{34}^{(1)} = 8.4(5)$ $\Delta_{diss}G^o = 5950(50) - 15.7(8)T$
complex	$T_{fusC} = 348.7 \pm 0.4$ $\Delta_{fus}H_C = 26850 \pm 800$	$T_{fusC} = 348.7(6)$ $\Delta_{fus}H_C = 26800(1000)$ $\Delta_fG^o_C = -28900(100) + 65.7(3)T$
	$T_{trs,II\rightarrow I,C} = 327.6 \pm 0.6$ $\Delta_{trs,II\rightarrow I}H_C = 2500 \pm 200$	$T_{trs,II\rightarrow I,C} = 327.7(1)$ $\Delta_{trs,II\rightarrow I}H_C = 1600(200)$
metatectic M_1	$T_{M1} = 327.6 \pm 1.0$ $x_{M1} = 0.22 \pm 0.01$	$T_{M1} = 327.7(3)$ $x_{M1} = 0.21(1)$
eutectic E_1	$T_{E1} = 318.4 \pm 0.5$ $x_{E1} = 0.16 \pm 0.02$ $\Delta_{fus}H_{E1} = 14100 \pm 900$	$T_{E1} = 318.4(2)$ $x_{E1} = 0.16(1)$ $\Delta_{fus}H_{E1} = 14000(100)$
eutectic E_2	$T_{E2} = 333.8 \pm 0.5$ $x_{E2} = 0.74 \pm 0.02$ $\Delta_{fus}H_{E2} = 14500 \pm 1200$	$T_{E2} = 333.7(2)$ $x_{E2} = 0.74(1)$ $\Delta_{fus}H_{E2} = 15040(50)$

product was purchased from Aldrich (purity > 96%) and was used without further purification. Impurities detected by coupling gaseous phase chromatography and mass spectrometry are $C_{10}HF_7$ (<1%), $C_{10}F_7Cl$ (<1%), and $C_{10}HF_6Cl$. A possible impact of such impurities is to displace liquidus lines in binary phase diagrams, in the $C_{10}F_8$ -rich regions.

This molecular compound gave rise to two different solid forms. Crystallographic data[12,20] are reported in Table 1 and thermodynamic data[12] in Table 2.

b. 2-Chloronaphathalene (or 2-$C_{10}H_7Cl$). The product was purchased from Fluka (purity higher than 98%). It presented a polymorphism with two phases: the phase transition is of the second order. Crystallographic data[2] are given in Table 1 and thermodynamic data in Table 2.

c. 2-Methylnaphthalene (or 2-$C_{10}H_7CH_3$). The product was purchased from Aldrich (purity 98%) and was used after a purification by sublimation, to minimize the content of 1-$C_{10}H_7CH_3$.[21] It presented two phase transitions of first order.[22] Only the parameters of the low-temperature form (III) and of the higher temperature form (I) are known[22] (Table 1). Thermodynamics data are reported in Table 2.

3.2. Binary Systems. *a. The 2-Chloronaphthalene−Octafluoronaphthalene System: Experimental Study.* This system presents a 1:1 complex with one first-order solid−solid transition. The thermodynamic behavior of this complex with congruent melting point and the data corresponding to invariant equilibria are given in Table 3. The consistency of the entire experimental data set allows us to establish the equilibrium phase diagram of the double-eutectic type (Figure 1).

The two solid complex phases (labeled II and I with increasing temperature) have been investigated by X-ray powder diffraction patterns at two temperatures (293 and 333 K); their monoclinic cell parameters and the proposed space groups are reported in Table 4 (phase II appears to be isomorphous with the low-

(20) Mackenzie, G. A., Buras, B.; Pawley, G. S. *Acta Crystallogr.* **1978**, *B34*, 1918.

(21) Meresse, A. Thesis, Université Bordeaux I, France, 1981.

(22) Meresse, A.; Chanh, N. B.; Housty, J.; Haget, Y. *J. Appl. Crystallogr.* **1983**, *16*, 370.

Table 4. Cell Parameters of the Complex 2-$C_{10}H_7Cl$:$C_{10}F_8$

phase	*a* (Å)	*b* (Å)	*c* (Å)	β (deg)	group	Z	V (Å^3)	*T* (K)
I	17.272(3)	6.698(3)	7.742(2)	99.90(3)	$P2_1/a$	2	882	333
II	12.717(3)	9.342(3)	7.408(2)	99.55(3)	$P2_1/a$	2	868	293

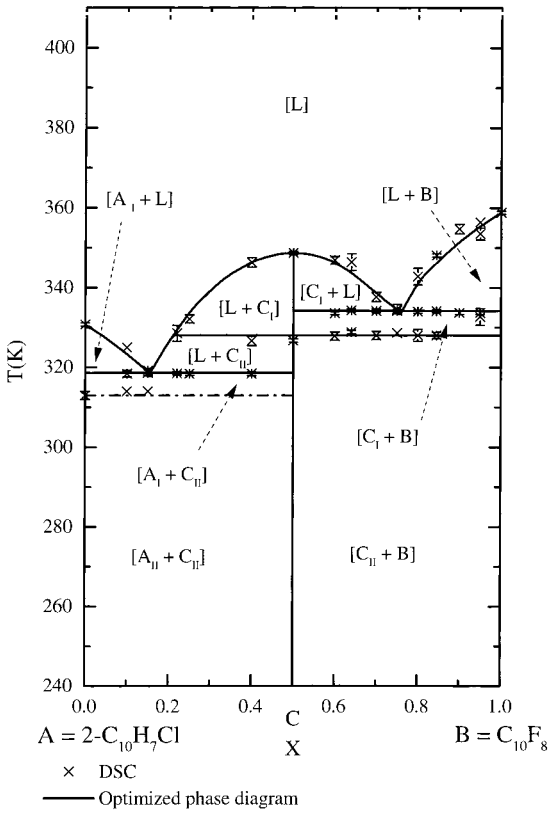

Figure 1. 2-Chloronaphthalene−octafluoronaphthalene system: experimental and calculated phase diagrams.

temperature phase of the homologous $C_{10}H_8$:$C_{10}F_8$ complex[23]).

Thermodynamic Analysis. SSM cannot describe this phase diagram. Therefore, the "BIMING" routine used liquid ASM, with five interaction parameters in eq 7: $H_{14}^{(1)}$, $H_{34}^{(1)}$, $S_{13}^{(1)}$, $S_{14}^{(1)}$, and $S_{34}^{(1)}$. The optimized values of invariant points are reported in Table 3. The calculated phase diagram is shown in Figure 1 (solid lines) and compared with the experimental data: the difference between experimental and calculated liquid molar fraction does not exceed 0.025 (the agreement was poorest in the octafluoronaphthalene-rich region).

At the complex melting temperature, the concentration of the associated species was $y_4 = 0.23$, showing strong intermolecular interactions in the liquid phase, although slightly weaker than in the homologous naphthalene−octafluoronaphthalene system ($y_4 = 0.28$,[12]). These results are in agreement with the corresponding Gibbs free energy of formation of complex phases at their melting point (−6.00 and −6.42 kJ mol^{-1},[12] respectively).

b. The 2-Methylnaphthalene−Octafluoronaphthalene System: *Experimental Study.* This system also presents a 1:1 complex with congruent melting point; therefore, the phase diagram will be again of the double-eutectic type. The study of equimolar mixtures with a Guinier-Simon camera showed four solid forms with increasing temperature, labeled δ, γ, β, and α (Figure 2). All the phase transitions are of the first order. The low-temperature form (δ) is stable at room temperature, the γ form exists between $T = 312$ and 324 K; the β form is present below $T = 329$ K, and the α phase exists above, until the melting temperature ($T = 383$ K). Only the α phase has an orthorhombic symmetry; the others (δ, γ, and β) are monoclinic. The cell parameters of these phases determined by powder diffraction are given in Table 5.

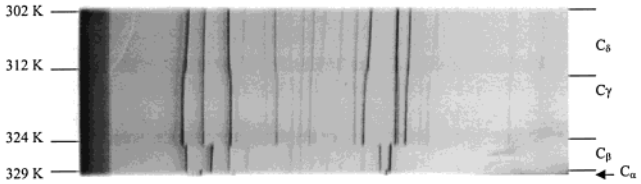

Figure 2. Guinier-Simon photograph showing the polymorphism of the 2-$C_{10}H_7CH_3$:$C_{10}F_8$ complex.

All the thermodynamic data of this binary system are given in Table 6. The consistency of the entire experimental data set allows us to establish the equilibrium phase diagram (Figure 3).

Thermodynamic Analysis. Liquid ASM is also needed for the thermodynamic analysis in this system (six interaction parameters are required: $H_{13}^{(1)}$, $H_{13}^{(2)}$, $H_{34}^{(1)}$, $S_{13}^{(1)}$, $S_{14}^{(1)}$, and $S_{34}^{(1)}$; see Table 6). Experimental and optimized values of all the invariant equilibria agree very well. The calculated phase diagram is shown in Figure 3; agreement between experimental and calculated liquidus lines is not so good. A possible explanation lies in the difficulty of controlling the 2-$C_{10}H_7CH_3$ composition, arising from the purity of both substances.

When the complex melts, the mole fraction of the associate ($y_4 = 0.16$) is lower than in the homologous with naphthalene ($y_4 = 0.28$[12]); at the same time, the Gibbs free energy of formation of the complex (−6.06 kJ mol^{-1}) is greater than for the homologous naphthalene complex (−6.42 kJ mol^{-1} [12]); once more, $C_{10}H_8$:$C_{10}F_8$ appears to be the most stable.

The effect of substitution on the aromatic ring on stability appears to be different in the benzene and naphthalene families: for the series R−C_6H_5:C_6F_6, where R ≃ H, Cl, and CH_3, Cl destabilizes the complex lattice of the pure hydrogenated complex, whereas CH_3 enhances the complex phases.[9−11] In contrast, for the naphthalene series 2R$C_{10}H_7$:$C_{10}F_8$, although Cl again seemed to have a destabilizing effect, the pure hydrogenated complex had the most stable lattice. One explanation may be that substitutions have a more "dilute" role in a naphthalene ring than in a benzene ring and thus less influence on the stability of the complex phases.

c. The 2-Chloronaphthalene−2-Methylnaphthalene System. This system is described elsewhere:[13,21−22] no complex phase is present, but a maximum appears in the phase diagram, which shows complete miscibility between pure components (Figure 4). Solid mixed alloys

(23) Potenza, J.; Mastropaolo, D. *Acta Crystallogr.* **1975**, *B31*, 2527.

Table 5. Cell Parameters of the Complex 2-$C_{10}H_7CH_3$:$C_{10}F_8$

phase	*a* (Å)	*b* (Å)	*c* (Å)	β (deg)	group	Z	V (Å^3)	*T* (K)
α	18.680(10)	6.229(6)	8.382(20)	90		2	975	333
β	17.550(2)	12.251(8)	8.441(5)	92.50(2)	$P2_1/a$	4	1806	328
γ	17.590(2)	6.856(2)	7.628(1)	98.79(2)	$P2_1/a$	2	909	323
δ	16.765(10)	7.083(6)	7.533(2)	96.92(3)	$P2_1/a$	2	888	293

Table 6. Comparison between Experiments and Optimization for the Thermodynamic Data of the 2-Methylnaphthalene−Octafluoronaphthalene System (SI units)

	experimental values	optimized values
liquid		$H_{13}^{(1)} = -1870(20)$ $S_{13}^{(1)} = -1.0(6)$ $H_{13}^{(2)} = -2400(50)$ $S_{13}^{(2)} = 0$ $H_{14}^{(1)} = 0$ $S_{14}^{(1)} = -23(5)$ $H_{34}^{(1)} = 220(10)$ $S_{34}^{(1)} = 49(5)$ $\Delta_{diss}G^o = 3270(100) - 65(1)T$
complex	$T_{fusC} = 382.7 \pm 0.6$ $\Delta_{fus}H_C = 21600 \pm 800$ $T_{trs,\beta\rightarrow\alpha,C} = 328.6 \pm 0.3$ $\Delta_{trs,\beta\rightarrow\alpha}H_C = 1600 \pm 400$ $T_{trs,\gamma\rightarrow\beta,C} = 323.7 \pm 0.3$ $\Delta_{trs,\gamma\rightarrow\beta}H_C = 5000 \pm 400$ $T_{trs,\delta\rightarrow\gamma,C} = 312.0 \pm 0.8$ $\Delta_{trs,\delta\rightarrow\gamma}H_C < 500$	$T_{fusC} = 382.7(6)$ $\Delta_{fus}H_C = 22000(1000)$ $\Delta_fG_C^o = -23100(100) + 45.0(8)T$ $T_{trs,\beta\rightarrow\alpha,C} = 329.0(1)$ $\Delta_{trs,\beta\rightarrow\alpha}H_C = 1600(200)$ $T_{trs,\gamma\rightarrow\beta,C} = 323.9(1)$ $\Delta_{trs,\gamma\rightarrow\beta}H_C = 5000(100)$ $T_{trs,\delta\rightarrow\gamma,C} = 312.4(1)$ $\Delta_{trs,\delta\rightarrow\gamma}H_C = 0$ $\Delta_{\delta\rightarrow\gamma}C_{Pc} = 15(2)$
eutectic E_1	$T_{E1} = 301.3 \pm 0.3$ $x_{E1} = 0.07 \pm 0.01$	$T_{E1} = 301.6(2)$ $x_{E1} = 0.07 \pm 0.01$
metatectic M_1	$T_{M1} = 312.0 \pm 0.8$ $x_{M1} = 0.08 \pm 0.02$	$T_{M1} = 312.4(2)$ $x_{M1} = 0.09(1)$
metatectic M_2	$T_{M2} = 323.7 \pm 0.3$ $x_{M2} = 0.11 \pm 0.02$	$T_{M2} = 323.9(2)$ $x_{M2} = 0.12(3)$
metatectic M_3	$T_{M3} = 328.6 \pm 0.3$ $x_{M3} = 0.12 \pm 0.03$	$T_{M3} = 329.0(2)$ $x_{M3} = 0.13(1)$
eutectique E_2	$T_{E2} = 338.7 \pm 0.3$ $x_{E2} = 0.78 \pm 0.01$	$T_{E2} = 339.0(1)$ $x_{E2} = 0.80(1)$

$Ax_1^sDx_2^s$ are in equilibrium with the ideal liquid. Calvet-Pallas et al.[13] have found the following expression for the excess solid functions:

$$\Delta_{mix}H_S(x_1^s, x_2^s) = x_1^s x_2^s[-2.60 + 0.52(x_1^s - x_2^s)] \quad \text{(in kJ mol}^{-1}\text{)}$$

$$\Delta_{xs}S_S(x_1^s, x_2^s) = x_1^s x_2^s[-2.5 + 0.5(x_1^s - x_2^s)] \quad \text{(in J mol}^{-1}\text{ K}^{-1}\text{)}$$

The present phase diagram type (continuous random alloys) is different from the preceding ones (ordered complex alloys): the presence of a maximum is the consequence of strong heteromolecular interactions in the lattice between 2-$C_{10}H_7Cl$ and 2-$C_{10}H_7CH_3$ molecules, which overcompensate the natural effect of the geometric mismatch,[13] whereas when one of the molecular partners in the lattice is $C_{10}F_8$, specific interactions enhance heteromolecular interactions, thus allowing ordering. Another reason continuous random alloys are not formed between $C_{10}F_8$ and one of the 2R-substitued naphthalene components is the lack of isomorphism between $C_{10}F_8$ and 2-$C_{10}H_7Cl$ or 2-$C_{10}H_7CH_3$;[2] therefore, in a mixed lattice, only ordering phase is possible. By using a modified pairwise approach, applied to different molecular substances (A, B) and to their binary aloys ($A_{1-x}B_x$),[8] we have recently shown that, even if homomolecular energies, ϵ°_{AA}, ϵ°_{BB}, and heteromolecular ones, ϵ°_{AB}, are of the same order, the difference of the lattice type (random alloys or ordered complexes) may be

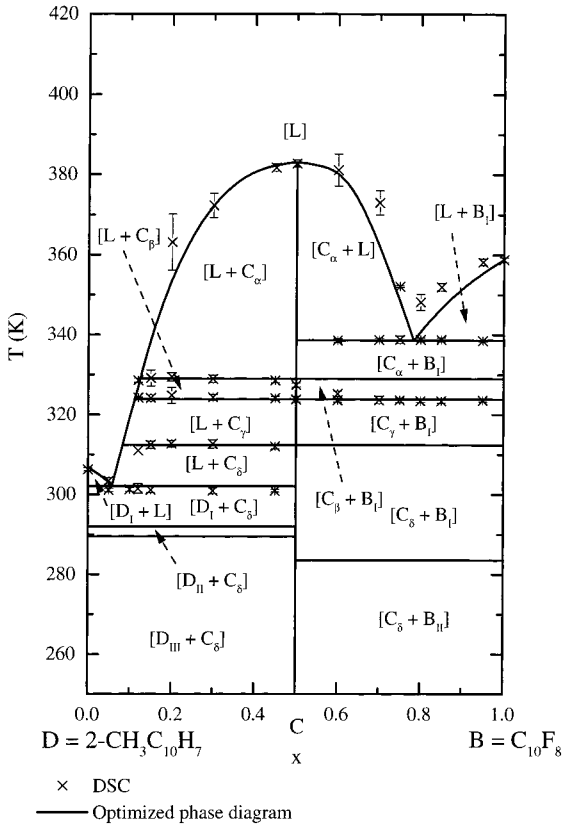

Figure 3. 2-Methylnaphthalene−octafluoronaphthalene system: experimental and calculated phase diagrams.

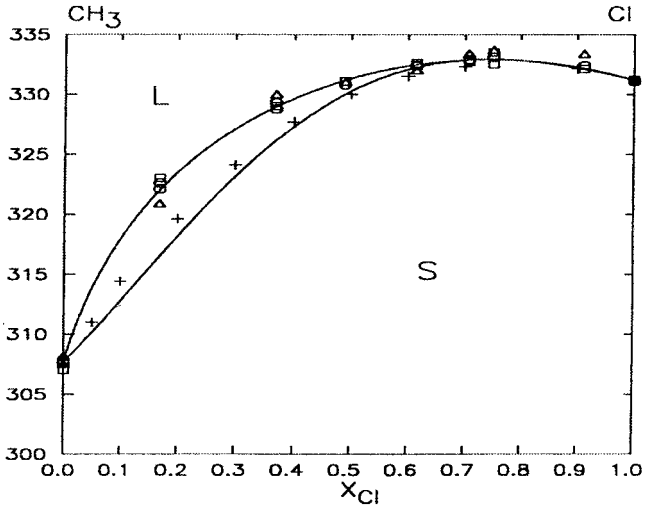

Figure 4. 2-Chloronaphthalene-2-methylnaphthalene system: phase diagram.

Table 7: Intermolecular Interaction and Long-Range Stabilizing Energies in Naphthalene Binary Systems (SI units) from Ref 17

	$zN\epsilon^{\circ}_{AB}$	$zN\epsilon^{\circ}_{AA}$ or $zN\epsilon^{\circ}_{BB}$	Φ_{AB}
2-$C_{10}H_7Cl$		−160200	
2-$C_{10}H_7CH_3$		−128000	
$C_{10}F_8$		−125200	
2-$C_{10}H_7Cl$−2-$C_{10}H_7CH_3$	−145900		
2-$C_{10}H_7Cl$:$C_{10}F_8$	−143900		5300
2-$C_{10}H_7CH_3$:$C_{10}F_8$	−130700		3900

explained by taking into account a stabilizing effect due to ordering, which is absent in random alloys. At 298 K, the corresponding quantity, Φ_{AB}, may be compared to $zN\epsilon^{\circ}_{AA}$, $zN\epsilon^{\circ}_{BB}$, and to $zN\epsilon^{\circ}_{AB}$ (z is the coordinence number and N is Avogadro's number). Table 7 shows that Φ_{AB} does not exceed 5% of homomolecular or heteromolecular quantities; nevertheless, this ratio is sufficiently large to allow long-range ordering.[8]

Another consequence of the differences between interactions, with and without complex formation, is that low contents of $C_{10}F_8$ in a ternary alloy, $(2\text{-}C_{10}H_7Cl)_{x_1^s}$-$(2\text{-}C_{10}H_7CH_3)_{x_2^s}(C_{10}F_8)_{x_3^s}$, would easily give a pseudobinary complex, $(2\text{-}C_{10}H_7Cl)_{1-x^s}(2\text{-}C_{10}H_7CH_3)_{x^s}$:$C_{10}F_8$.

3.3. Ternary System: 2-$C_{10}H_7Cl$−2-$C_{10}H_7CH_3$−$C_{10}F_8$. Before studying the ternary phase diagram, we examined its pseudobinary section corresponding to the composition in $C_{10}F_8$, $x_3 = 0.5$.

a. The Pseudobinary {(1 - z)/2[2-$C_{10}H_7Cl$ + $C_{10}F_8$] + z /2[2-$C_{10}H_7CH_3$ + $C_{10}F_8$]}: Experimental Study. An experimental phase diagram, deduced from 11 compositions ($x_2 = z = 0.1$, 0.2, 0.3, 0.4, 0.45, 0.5, 0.6, 0.7, 0.8, 0.9, and 0.95) analyzed by DSC and by X-ray powder diffraction, is given in Figure 5: four invariant equilibria are found; three of them [a peritectic at (350.6 ± 0.5) K, a peritectoïd at (327 ± 1) K, and a eutectoïd at (287 ± 1) K] are the result of the polymorphism of both complexes, 2-$C_{10}H_7Cl$:$C_{10}F_8$ and 2-$C_{10}H_7CH_3$:$C_{10}F_8$. All solid phases are of the type $(2\text{-}C_{10}H_7Cl)_{1-x^s}$ $(2\text{-}C_{10}H_7CH_3)_{x^s}$:$C_{10}F_8$.

In the higher temperature part, phase α, which is isomorphous with the α form of the 2-$C_{10}H_7CH_3$:$C_{10}F_8$ complex, is present in a large composition range, from $x^s = 0.12$ up to $x^s = 1$. Diffraction patterns show syncrystallization between phase I (the higher temperature form of the 2-$C_{10}H_7Cl$:$C_{10}F_8$ complex) and the γ phase of the 2-$C_{10}H_7CH_3$:$C_{10}F_8$ complex: the continuity of cell parameters versus composition, for temperatures around 330 K, means that phases I and γ are isomorphous (Figure 6). It may be remembered that 2-$C_{10}H_7CH_3$:$C_{10}F_8$ in the γ phase is not stable at 330 K; therefore, diffraction patterns of 2-$C_{10}H_7CH_3$:$C_{10}F_8$ are recorded, in fact, at 325 K. Excess volume, $\Delta_{xs}V_\gamma$, can be expressed as a Redlish-Kister polynomial form:

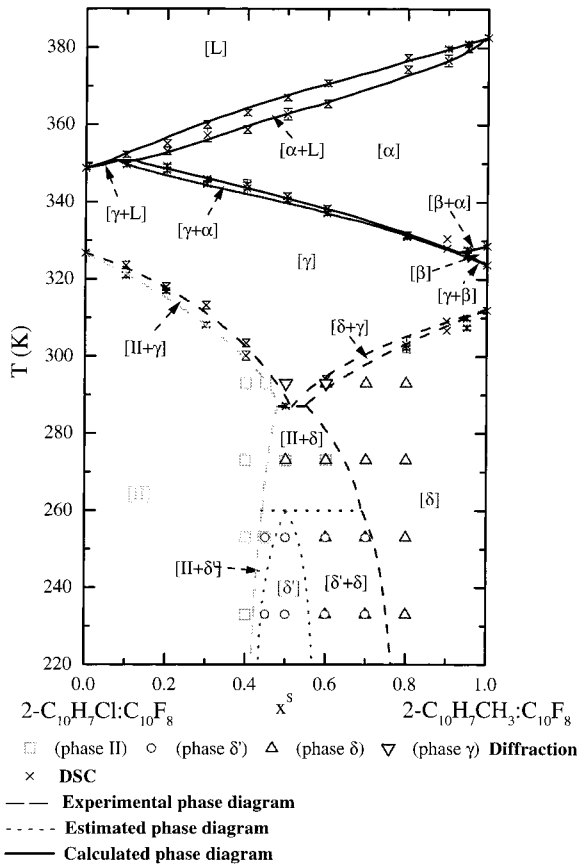

Figure 5. 2-Chloronaphthalene−2-methylnaphthalene−octafluoronaphthalene system: pseudobinary section.

$$\Delta_{xs}V_\gamma = x^S(1 - x^S)\ 21.4 \quad (\text{in cm}^3\ \text{mol}^{-1})$$

Consequently, (i) phase I will be referred to as γ from now on, and (ii) $\Delta_{mix}H_\gamma$ also will be positive. The evolution of the enthalpy, $\Delta_{trs,\ \gamma\rightarrow\alpha}H$, is reported in Table 8.

At low temperatures, between phase II of the 2-$C_{10}H_7Cl$:$C_{10}F_8$ complex and phase δ of the 2-$C_{10}H_7CH_3$:$C_{10}F_8$ complex, a miscibility gap occurs around the composition $x^s = 0.5$; for example, Figure 7 shows the evolution of the cell parameters versus composition at $T = 293$ K: there is no isomorphism between these two phases.

Below 260 K, there was a new phase, labeled δ′. Its diffraction patterns differ from those of the δ phase ones only in some supplementary reflections. We cannot index the δ′ diffraction patterns, because kinetic effects probably do not allow an entire transformation of δ into δ′. Therefore, the stability domain of δ′ may be only estimated; because of the central position of δ′, this phase is probably ordered.

Table 8. Thermodynamic Data (experiments and optimization) in the Pseudobinary Section between 2-$C_{10}H_7Cl$:$C_{10}F_8$ and 2-$C_{10}H_7CH_3$:$C_{10}F_8$ Complexes (SI units)

	experimental values	optimized values
liquid		$H_{15}^{(1)} = 5330(50)$, $H_{24}^{(1)} = 2060(100)$ $H_{123} = -400(100)$
complex 2-$C_{10}H_7Cl$:$C_{10}F_8$		"$T_{fus,\alpha}$" = 346.9(8) "$\Delta_{fus}H_\alpha$" = 19300(50) "$T_{trs,\gamma\to\alpha}$" = 353.3(8) "$\Delta_{trs,\gamma\to\alpha}H$" = 7540(50)
complex 2-$C_{10}H_7CH_3$:$C_{10}F_8$	$T_{trs,\gamma\to\alpha} = 324.9 \pm 0.5$ $\Delta_{trs,\gamma\to\alpha}H = 6600 \pm 800$	
peritectic	$T_p = 350.6 \pm 0.5$ $x_p = 0.06 \pm 0.01$ $x_{p,\gamma}^S = 0.08 \pm 0.02$ $x_{p,\alpha}^S = 0.12 \pm 0.02$	$T_p = 350.7(3)$ $x_p = 0.060(5)$ $x_{p,\gamma}^S = 0.080(5)$ $x_{p,\alpha}^S = 0.116(5)$
pseudobinary solids		
	$\Delta_{trs,\gamma\to\alpha}H$	$\Delta_{trs,\gamma\to\alpha}H$
$x^S = 0.2$	7300 ± 200	7270(10)
$x^S = 0.3$	7200 ± 400	7100(20)
$x^S = 0.4$	7000 ± 400	7050(20)
$x^S = 0.5$	6900 ± 200	6900(30)
$x^S = 0.6$	6600 ± 200	6850(20)
$x^S = 0.8$	6800 ± 100	6720(20)
phase α		$H_\alpha^{(1)} = 1840(50)$, $H_\alpha^{(2)} = -490(10)$
phase γ		$H_\gamma^{(1)} = 2520(50)$, $H_\gamma^{(2)} = 0$

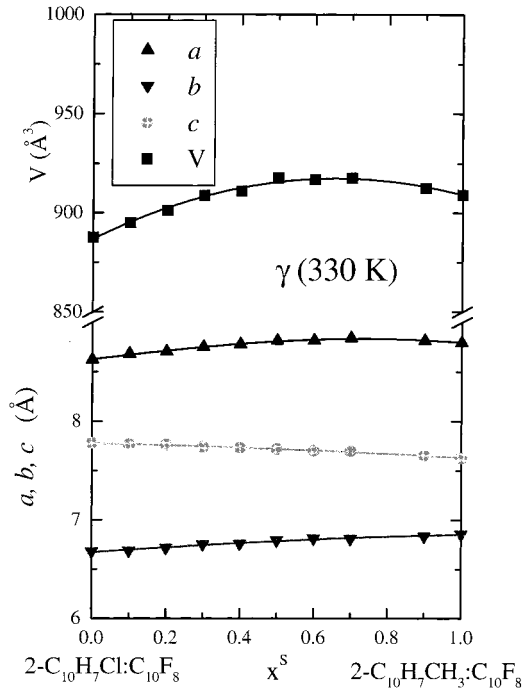

Figure 6. Evolution of the cell parameters in the γ phase at $T \approx 330$ K: isomorphism between the high-temperature form of 2-$C_{10}H_7Cl$:$C_{10}F_8$ and the γ form of 2-$C_{10}H_7CH_3$:$C_{10}F_8$.

Thermodynamic Optimization. The optimization concerns the equilibrium α⇔L, γ⇔L, γ⇔α, for which experimental data are sufficient. The ASM model was used to describe the liquid phase, with the uncombined species 1 (A), 2 (D), and 3 (B) and the associated ones 4 (A:B) and 5 (D:B). According to eq 7, new parameters, which were not present in the constituting binaries, must be taken into account in the modeling of the liquid mixing properties. If we restrict calculation to enthalpic terms of the first order, we should have four parameters: $H_{15}^{(1)}$, $H_{24}^{(1)}$, $H_{45}^{(1)}$ and a ternary term, H_{123}. Since association is weak in 1−4 and 2−3 binaries, the influence of interactions between associated species can be neglected and, therefore, the new liquid parameter set reduces to $H_{15}^{(1)}$, $H_{24}^{(1)}$, and H_{123}. To minimize the number of solid-phase parameters (α and γ), no excess entropy is taken into account ($\Delta_{xs}S_\alpha$, $\Delta_{xs}S_\gamma = 0$ in eq 6).

By using "TERMING",[19] the optimization procedure is started by analyzing solid−solid equilibrium between α and γ phases (temperatures, $T_{trs,\ \gamma\to\alpha}$, and enthalpies of transition, $\Delta_{trs,\ \gamma\to\alpha}H$). The resulting parameters, $H_\alpha^{(1)}$, $H_\alpha^{(2)}$, $H_\gamma^{(1)}$, and $H_\gamma^{(2)}$, are given in Table 8. The final values of $\Delta_{trs,\gamma\to\alpha}H$ are also reported with special attention to the metastable phase α of 2-$C_{10}H_7Cl$:$C_{10}F_8$ ("$T_{fus,\alpha}$" = 346.9 K, "$\Delta_{fus,\alpha}H$" = 19 300 J mol^{-1}); in agreement with experimental values, they lead to a narrow loop and to a negative difference between the Gibbs free energy of each phase ($\Delta_{trs}G_{\gamma\to\alpha}$ equals 170 J mol^{-1} at $x^s = 1/2$.

All of these parameters are then used for analyzing equilibria α⇔L or γ⇔L; finally, liquid parameters are given in Table 8, and the calculated upper part of the pseudobinary section of the ternary phase diagram is shown in Figure 5 (continuous lines): differences between experimental and calculated compositions do not exceed $\Delta x_2 = 0.02$ and $\Delta x^s = 0.04$ for equilibria α⇔L or γ⇔L, and $\Delta x^s = 0.03$ for equilibrium γ⇔α. The calculated peritectic invariant corresponding to equilibrium γ⇔α + L is also in good agreement with measurements.

The presence of pseudobinary disordered alloys between the two limiting complexes, 2-$C_{10}H_7Cl$:$C_{10}F_8$ and 2-$C_{10}H_7CH_3$:$C_{10}F_8$, may be the consequence of a stabilizing influence of $C_{10}F_8$, which enhances heteromolecular interactions in the mixed lattice. It may also be assumed that this stabilizing influence affects neighboring molecules, which may lead to a pseudobinary ordered lattice for $x^s = 1/2$: in other words, δ' phase may behave as a "complex of complexes"!

b. The Ternary System. Experimental Study. Some points inside the Gibbs triangle corresponding to $x_1/x_2 = 1$ compositions have been prepared: $x_3 = 0.1$, 0.3, 0.5, and 0.7. Experimental liquidus temperatures are respectively $T = (324 \pm 0.7)$, (357 ± 1), (367.0 ± 0.7), and (338.0 ± 0.7) K. The first point corresponds to an

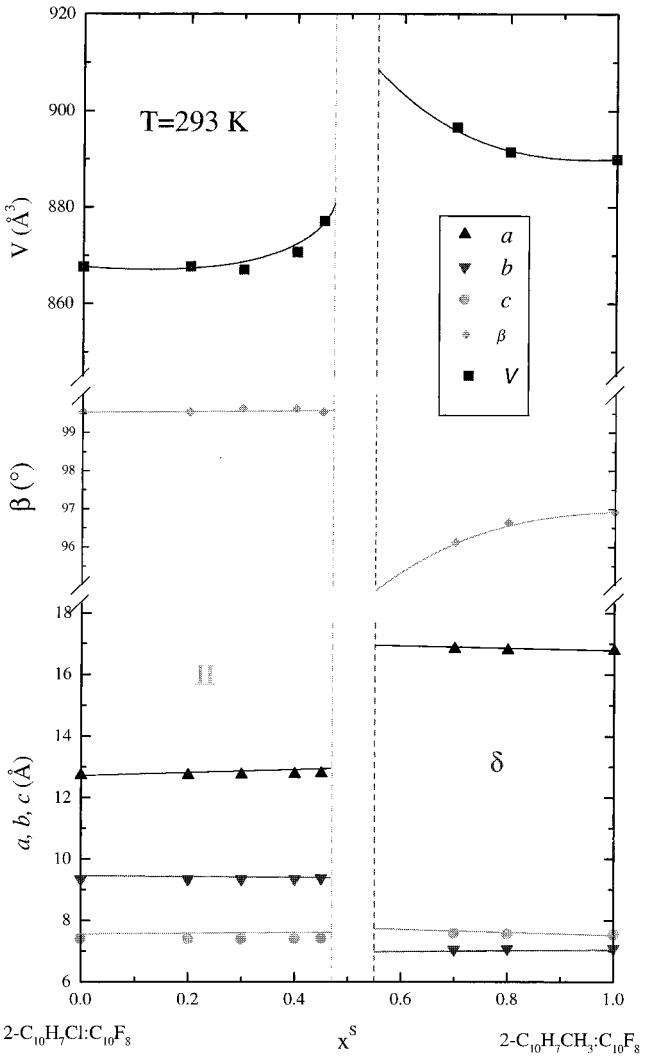

Figure 7. Evolution of the cell parameters in the II form of 2-$C_{10}H_7Cl$:$C_{10}F_8$ and of the δ form of $C_{10}H_7CH_3$:$C_{10}F_8$ at T = 293 K: these phases have the same symmetry, but they are not isomorphous.

equilibrium between L and a disordered ternary alloy, $(2\text{-}C_{10}H_7Cl)_{x_1^s}(2\text{-}C_{10}H_7CH_3)_{x_2^s}(2\text{-}C_{10}F_8)_{x_3^s}$, isomorphous with the high-temperature form of 2-$C_{10}H_7Cl$. For the other points, the solid phase is a pseudobinary complex, in the α or γ form.

Calculated Liquidus Surface. With the entire parameter set of L, γ, and α phases, we are able to predict the liquidus surface corresponding to the $\alpha \Leftrightarrow$L and $\gamma \Leftrightarrow$L equilibria. As shown by Figure 8, six isothermal sections of this surface (continuous lines) have been calculated. Our approach is supported by finding that experimental

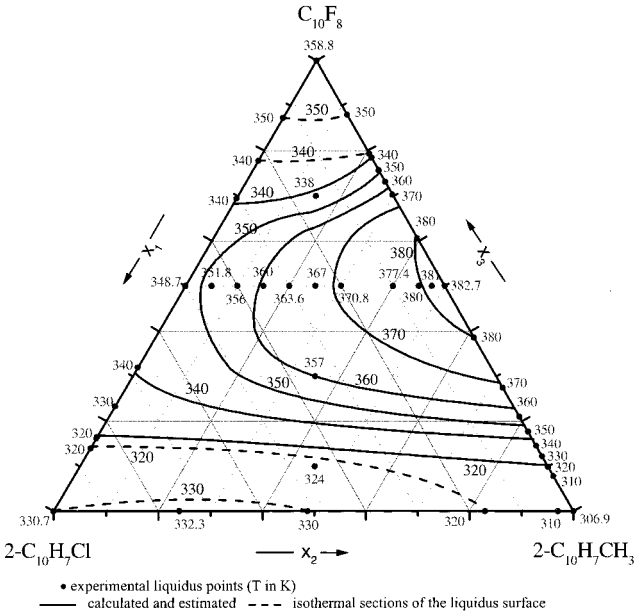

Figure 8. 2-Chloronaphthalene−2-methylnaphthalene−octafluoronaphthalene system: isothermal sections of the liquidus surface (T = 320, 330, 340, 350, 360, 370, and 380 K).

points are located well on the network of these isothermal lines. Because "TERMING" cannot study equilibria involving disordered ternary alloys, no calculation of the 2-$C_{10}H_7Cl$−2-$C_{10}H_7CH_3$-and of the $C_{10}H_8$-rich parts of the phase diagram has been made. Therefore, only extrapolated isothermal sections (dashed lines) from the three constituting binary systems are shown in Figure 8.

4. Conclusion

The optimization of the liquid phase, in the 2-chloronaphthalene−2-methylnaphthalene−octafluoronaphthene system, required the associated solution model to explain liquid properties, with strong intermolecular interactions. We have shown the isomorphism between the phase I of the 2-chloronaphthalene:octafluoronaphthalene complex and the phase γ of the 2-methylnaphthalene:octafluoronaphthalene complex. In the low-temperature range of the pseudobinary section (octafluoronaphthalene content = 1/2), a new phase appears in the middle of the phase diagram, probably corresponding to an ordered phase. With a low content of octafluoronaphthalene, disordered ternary alloys are not stable, whereas pseudobinary complex alloys show the influence of specific interactions due to F-atoms, which enhance classical van der Waals forces.

CM001046U